Terr. Atmos. Ocean. Sci., Vol. 20, No. 2, 333-343, April 2009 doi: 10.3319/TAO.2008.02.04.01(A)

A Study of East Asian Cold Surges during the 2004/05 Winter: Impact of East Asian Jet Stream and Subtropical Upper-Level Rossby Wave Trains

Chi-Cherng Hong[1, *], Huang-Hsiung Hsu[2], and Hsin-Hsing Chia[3]

[1] *Department of Science, Taipei Municipal University of Education, Taipei, Taiwan, ROC*
[2] *Department of Atmospheric Science, National Taiwan University, Taipei, Taiwan, ROC*
[3] *Central Weather Bureau, Taipei, Taiwan, ROC*

Received 19 June 2007, accepted 4 February 2008

ABSTRACT

Cold surges were unusually active in subtropical East Asia during January - February 2005. These cold surges were preceded by upstream wave trains, which originated in the Mediterranean-Sahara region and propagated eastward along the subtropical jet stream over the Eurasian continent. The northerly of the upper-level cyclonic anomaly in East Asia coupled with the low-level northerly upon the arrival of wave activity, and this was followed by a quick southward penetration of cold air mass and surface anticyclone. Diagnostic and numerical results suggest that the anomalously active wave activity affecting the East Asian cold surges may be attributed to an anomalously enhanced jet stream over the Middle East and an anomalously westward extension of the East Asian Jet Stream. The configuration of these two subtropical jet streams established a strong waveguide through which wave activity forced in the Mediterranean-Sahara region could efficiently propagate to East Asia, resulting in above average cold surge events in subtropical East Asia. Wave-like perturbation tended to be amplified at the entrance to the East Asian jet through barotropic energy conversion from the mean flow.

Key words: Cold surges, Wave trains, Jet stream

Citation: Hong, C. C., H. H. Hsu, and H. H. Chia, 2009: A study of East Asian cold surges during the 2004/05 winter: Impact of East Asian Jet Stream and subtropical upper-level rossby wave trains. Terr. Atmos. Ocean. Sci., 20, 333-343, doi: 10.3319/TAO.2008.02.04.01(A)

1. INTRODUCTION

The East Asian cold surge is one of the most prominent phenomena in the East Asian winter monsoon. The cold surge, accompanied by strong northerly winds, causes not only natural disasters in East Asia, but also brings monsoon rainfall to Southeast Asia (Boyle and Chen 1987). There are two types of cold surges over East Asia, namely the easterly surge and the northerly surge (Wu and Chan 1995). Cold air and surface anticyclone in a cold surge event often move southward along the eastern periphery of the mountains east of the Tibetan Plateau from Siberia to Southern China, Taiwan, and even the South China Sea in some strong events (e.g., Lau and Lau 1984; Hsu 1987; Compo et al. 1999). Taiwan, an island off the southeastern coast of China, was affected by this southward-penetrating cold surge 2.5 times per winter from 1981 - 2000 (Wu et al. 2007). However, in the 2004/2005 winter, four cold surges reached Taiwan. This unusually strong cold surge activity broke a 40-year record and caused significant agriculture loss in Taiwan.

Previous studies have revealed that East Asian cold surges are often preceded by upstream upper-level disturbances originating in the western Eurasian continent (Joung and Hitchman 1982; Wu and Chan 1997; Chen et al 2002). Similarly, the four cold surge events in the 2004/05 winter were preceded by wave-like disturbances propagating eastward from Europe to East Asia along the subtropical jet stream, which has been identified as a Rossby waveguide in previous studies (e.g., Hsu and Lin 1992; Hoskins and Ambrizzi 1993). Through this jet-stream waveguide Asia weather can be affected by, forcing or perturbation occurring as far upstream as Europe in just a few days.

* *Corresponding author*
E-mail: cchong@tmue.edu.tw

Despite this knowledge of upstream wave-like disturbances, the mechanism guiding the wave train has not been fully explored. In view of strong cold surges and upstream wave activity in the 2004/2005 winter, this study aims to explore the waveguide effect on wave-like disturbances in the upper troposphere and the possible effect of upper-level wave activity on the initiation of cold surges in the 2004/05 winter. In this study, we will demonstrate that upper-level Rossby wave trains originating in the Mediterranean-Sahara region and propagating through the jet-stream waveguide helped trigger the East Asian cold surge. It is also suggested that the East Asian Jet Stream (EASJ) plays an important role in amplifying the wave-like disturbances through wave-mean flow interaction. Numerical simulation will also demonstrate the sensitivity of the wave propagation to the detailed structure of the subtropical jet stream.

2. DATA AND MODEL

Daily NCEP/NCAR reanalysis wind, geopotential height (Kalnay et al. 1996) during the 2004/05 winter are used in this study. Cold surges were identified based on criteria defined by the Central Weather Bureau, the official meteorological agency of Taiwan. The criteria are: (i) the daily maximum temperature of Taipei (located in northern Taiwan) drops at least 4 C within 24 - 48 hours; and (ii) the daily minimum temperature is less than 10 C. To make sure the cold surge is not station dependent, the data of Pengchiayu, an island to the northeast of Taipei, is also used to identify cold surges. Four cold surge events listed in Table 1 were identified. The corresponding time series of daily minimum temperature is also shown in Fig. 1. The abrupt temperature drop ranges from 4.8 to C and the minimum temperature fell to 7.3 - 9.6 C. It is also interesting to note that the cold surges occurred regularly every 16 - 18 days after a warm December.

The model used to explore the waveguide effect on Rossby wave-like disturbances is a linearized perturbation barotropic vorticity equation. It is outlined as:

$$\partial\zeta' / \partial t = -V' \cdot \nabla(\overline{\zeta} + f) - \overline{V} \cdot \nabla\zeta' - k\zeta' - r\nabla^4\zeta' + s' \quad (1)$$

where, prime represents the anomaly deviation from monthly climatology, over bar denotes the climatological mean variable, ζ the 200-hPa relative vorticity, V two dimensional wind, f the Coriolis parameter, $k\zeta$ Rayleigh (linear) drag term, r $^4\zeta$ biharmonic diffusion, and s vorticity forcing. The coefficients for Rayleigh friction and biharmonic diffusion are 3.935 10^{-7} s^{-1} (equivalent to a 10-day damping) and 2 10^{16} m^4 s^{-1}, respectively. The model is a nondivergent global spectrum model with a T42 horizontal resolution (128 64). Previous tests show that this model simulates well Rossby wave propagation either for the initial or forced problem (Hsu 1994). In the following experiments, a prescribed elliptical forcing (s), the Rossby wave source (RWS, Sardeshmukh and Hoskins 1988), calculated from observation is added to Eq. (1). The RWS was multiplied by 10^{-5} to make the simulation essentially linear. Three sets of mean flows at 200 hPa, i.e., the climatological zonal mean flow (here after climz_exp), climatological time mean flow (hereafter clim_exp) and the mean flow in January - February 2005 (hereafter surge_exp), were used as basic flow in the numerical experiments to explore the waveguide effect of the basic flow on the perturbation.

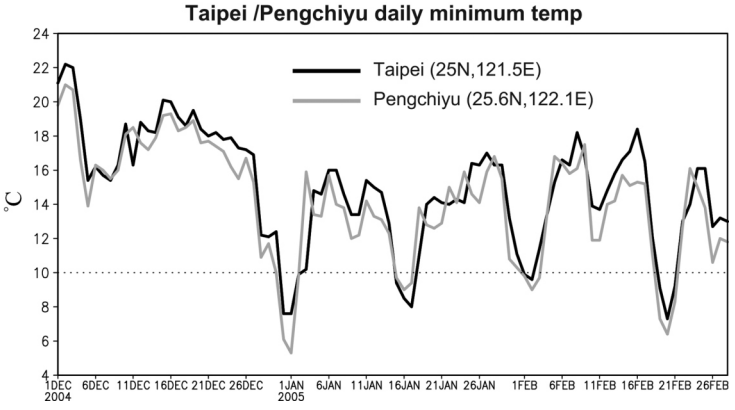

Fig. 1. Time series of the daily minimum temperature of Taipei (dark line) and Pengchiayu (gray line) during the 2004/05 winter. Daily minimum temperature below 10 C (dash line) is defined as a cold surge.

Table 1. Dates of the East Asian cold surges in the 2004/05 winter and the corresponding temperature drop within 24 - 48 hours (column 3) and minimum temperature (column 4) in Taipei.

Cold surge	Periods	ΔT_{max} (24 - 48 h)	T_{min} (°C)
case 1	12/29, 2004 - 1/2, 2005	9.9	7.6
case 2	1/14, 2005 - 1/17, 2005	4.8	8
case 3	2/1, 2005 - 2/3, 2006	6.9	9.6
case 4	2/19, 2005 - 2/21, 2006	9.9	7.3

3. COLD SURGE AND UPSTREAM WAVE ACTIVITY

Figure 2 shows the 200-hPa wind and the 850-hPa temperature anomalies on the first day of cold surge defined by Table 1. An upper wave-like wind anomaly appearing in the subtropical jet is observed for all four events. The distributions of negative temperature anomalies (shading) seem to indicate that the southward penetration of cold air mass along the lee side of Tibetan Plateau is accompanied

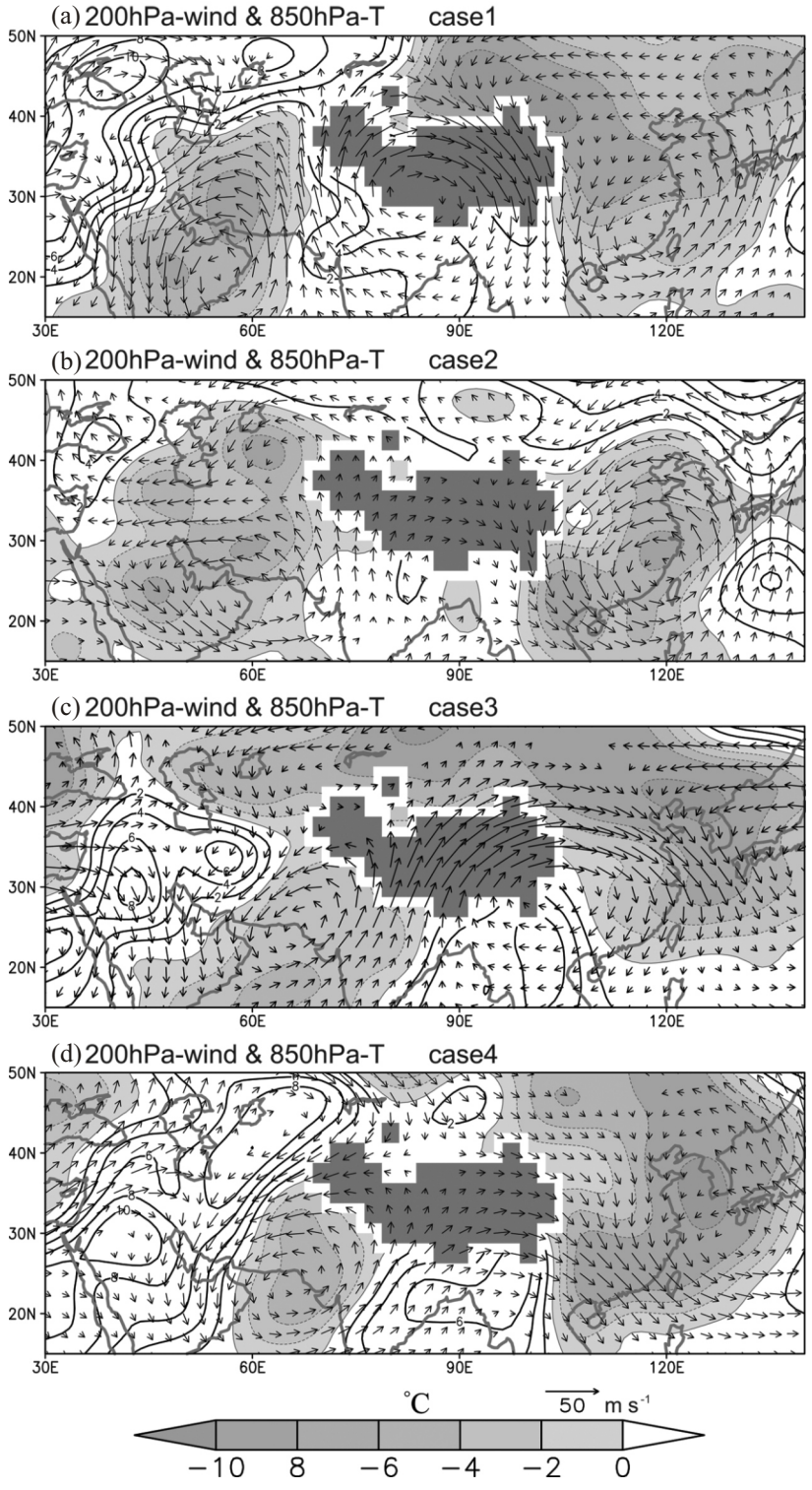

Fig. 2. 200-hPa wind and 850-hPa temperature anomalies (contour) on the first day of four cold surge events defined in Table 1. Contour interval is 2 C and negative temperature anomaly is shaded.

by the arrival of the northerly anomalies aloft. To further demonstrate the relationship between the upper and low-level wind anomalies, a longitude-height cross section of meridional wind anomaly averaged over 20 - N is shown in Fig. 3. Zonal wind is also plotted to indicate the existence of two jet streams: the EASJ and another one over the Middle East. The figure reveals a wave-like structure with zonal scale equivalent to zonal wavenumber 6 in all cold surge events (Fig. 3). The wave-like patterns exhibit equivalent barotropic vertical structure with the largest amplitude in the upper troposphere. Particularly interesting is the region of northerly anomaly near the East Asian coast. The northerly anomaly exists from the upper troposphere to near the surface and coincides with the southward penetration of cold air and the low-level northerly embedded in the cold surges. An examination of the temporal evolution of each cold surge event indicates that the region of the near-surface northerly started moving southward upon the arrival of the wave-like disturbance. This seems to suggest that the northerly in the wave-like disturbance helped trigger the southward advance of cold surge. This is consistent with the coupling of the upper trough with low-level circulation reported by Chen et al. (2002). One example will be shown and discussed in Fig. 5.

The temporal evolution of these four wave-like disturbances is shown in Fig. 4, which presents the Hovmüller diagram of 200-hPa meridional wind anomaly averaged over 20 - N. There are many wave-like patterns, which are characterized by the intermittently positive and negative meridional wind anomalies from 0 to 120 E and by the sequential development of a new anomaly center in the downstream. But only four events, indicated by the dashed arrows, exhibit northerly anomaly at the most eastern end of these wave-like structures. Also plotted in contours is the meridional wind anomaly at 850 hPa between 80 and E. It is interesting that the northerly anomaly at 850 hPa is also observed only during the four cold surge events. Note that the northerly anomaly in early December is not accompanied by a cold surge because of the warm December (Fig. 1) and the weak Siberian High. The above features also suggest that the cold surges occurred upon the arrival of wave activity, which propagates eastward from northern Africa (Sahara) to East Asia.

To understand how wave activity propagates, the wave activity flux (WAF) defined by Takaya and Nakamura (2001) was computed. Here only the WAF and the corre-

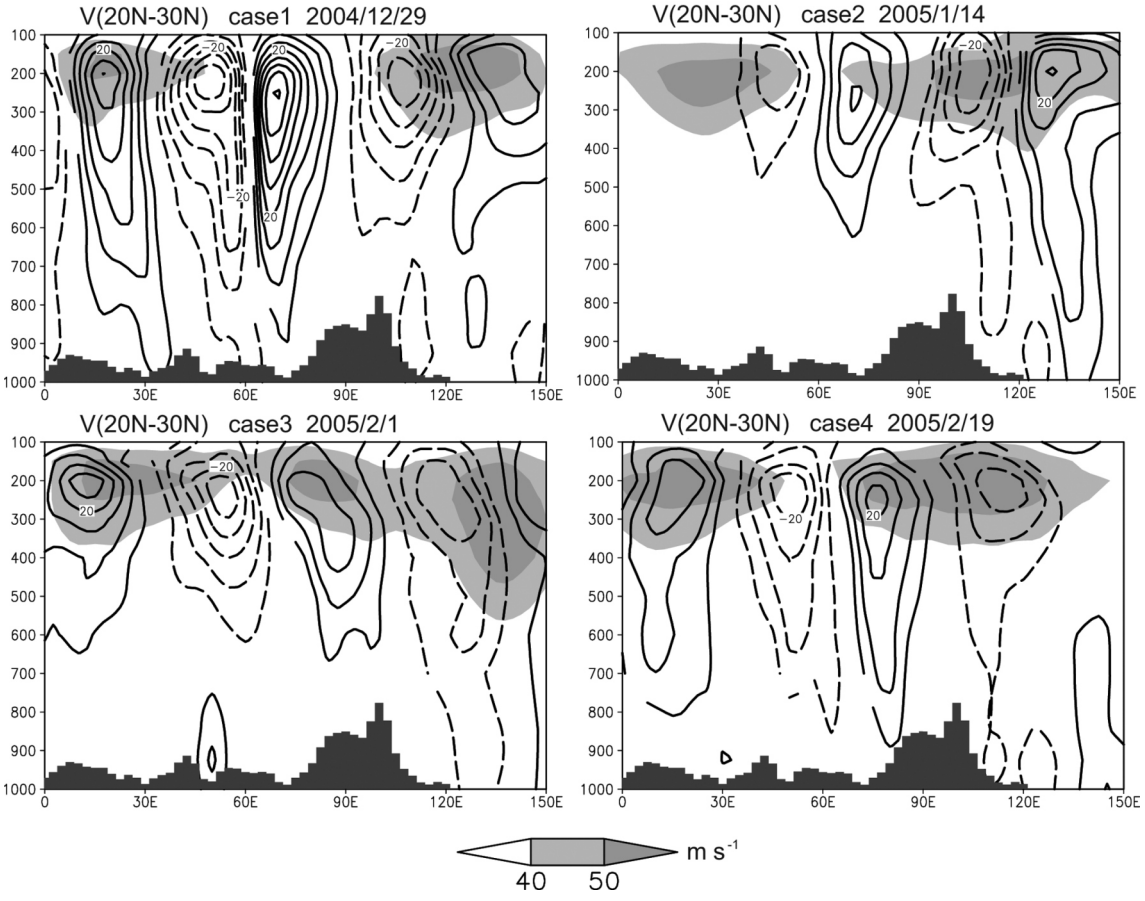

Fig. 3. Same as in Fig. 2, but for the longitude-height cross section of anomalous meridional wind (averaged over 20 - N). Dark bar and gray shading denote topography and total zonal wind, respectively. Contour represents meridional wind anomaly with 5 m s^{-1} interval.

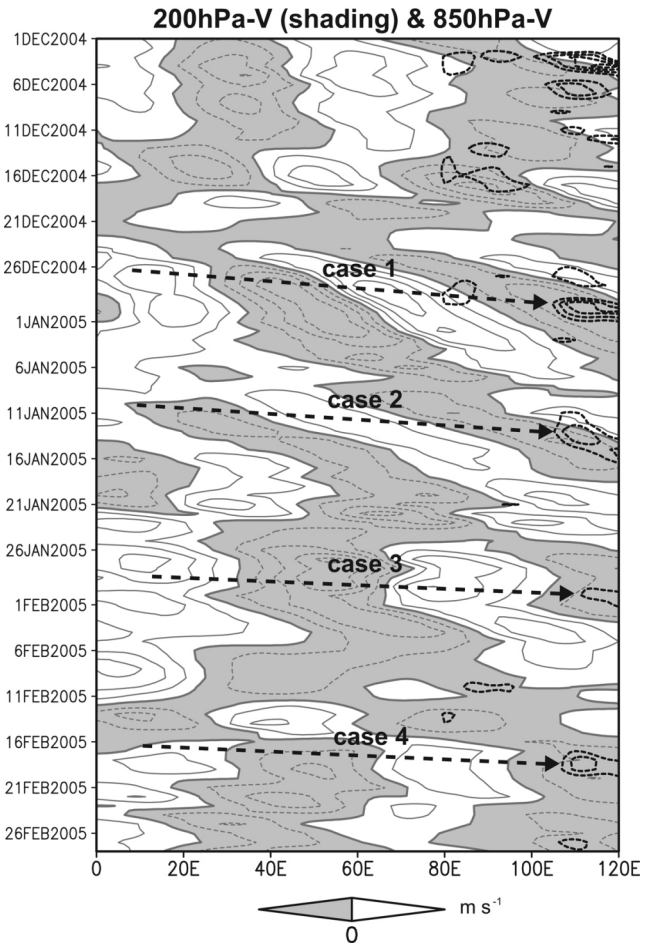

Fig. 4. Hovmüller diagrams of the 200-hPa (shading) and 850-hPa (contour) meridional wind anomaly averaged over 20 - N. Only the 850 hPa northerly anomaly in East Asia (80 - E) less than -3 m s^{-1} is plotted. Contour interval is 3 m s^{-1}. Dashed arrows denote the wave trains linked with cold surges.

sponding stream function anomaly at 200 hPa for the first cold surge are shown in Fig. 5. The other cases exhibit similar characteristics. Figure 5a reveals significant wave activity flux from the Mediterranean-Sahara to the Middle East 5 days before the onset of cold surge in Taiwan. Continuous eastward propagation of wave activity and development of new centers of action along the subtropical jet are evident at Day -3 (Fig. 5b). By Day -1, a cyclonic anomaly appeared over eastern China while the WAF had further extended into the western North Pacific. This series indicates the eastward energy dispersion of the Rossby wave-like disturbances through the subtropical jet-stream waveguide from the Mediterranean-Sahara to East Asia in only four days. The right panels of Fig. 5 represent the corresponding sea level pressure and 850-hPa temperature at Day -5, -3, and -1. The cold air mass and the anticyclone did not move quickly southward toward Taiwan until Day -3 to -1 when the cyclonic anomaly over eastern China developed and the WAF arrived at East Asia. This sequence demonstrates again that this cold surge was closely related to the upper-tropospheric wave activity originating in the Mediterranean-Sahara region.

A close examination of Fig. 5 reveals that the disturbances tend to amplify at the entrance of the EAJS, e.g., the amplitudes of the positive anomaly over northern India and the negative anomaly over eastern China increased from Day -3 to -1. As noted above, the northerly over eastern China was enhanced in the whole troposphere and cold air mass started moving southward upon the arrival of the wave-like disturbances. Amplification of the disturbances may provide the extra push to the occurrence of cold surge.

4. BAROTROPIC KINETIC ENERGY CONVERSION

Both barotropic and baroclinic instability could contribute to the amplification of disturbances through wave-mean flow interaction. Considering the barotropic nature of the disturbances, the following discussion will focus on the barotropic part, although the contribution of the baroclinic component may not be negligible. Following Simmons et al. (1983), we diagnose barotropic kinetic energy conversion of disturbances to understand how the EAJS influences the amplitude of disturbances.

The barotropic perturbation kinetic energy equation can be written as:

$$\begin{aligned} \partial KE / \partial t \;=\; & -u'v'(\partial \overline{u} / \partial y) \;-\; u'v'(\partial \overline{v} / \partial y) \\ & +\,(v'^2 \;-\; u'^2)(\partial \overline{u} / \partial x) \\ & -\; v'^2(\partial \overline{u} / \partial x \;+\; \partial \overline{v} / \partial y) \end{aligned} \qquad (2)$$

where, $KE = (u^2 + v^2) / 2$ represents the perturbation kinetic energy, (u , v) denotes horizontal wind perturbation, the over bar indicates the climatological mean. As the climatological-mean wind is nearly non-divergent and the zonal wind shear ($\overline{u} / y$) is much larger than meridional wind shear ($\overline{v} / y$), the perturbation kinetic energy equation can be approximated by:

$$\partial KE / \partial t \;\simeq\; -u'v'(\partial \overline{u} / \partial y) \;+\; (v'^2 \;-\; u'^2)(\partial \overline{u} / \partial x) \qquad (3)$$

The first term ($u\,v\;\overline{u} / y$) in the right hand side corresponds to the meridional shear instability of zonal mean flow, and the second term ($v^2 \;\; u^2$) $\overline{u} / x$ corresponds to the zonally asymmetric instability of zonal mean wind, which becomes important when the disturbance passes through jet stream.

Both terms were calculated and the values averaged

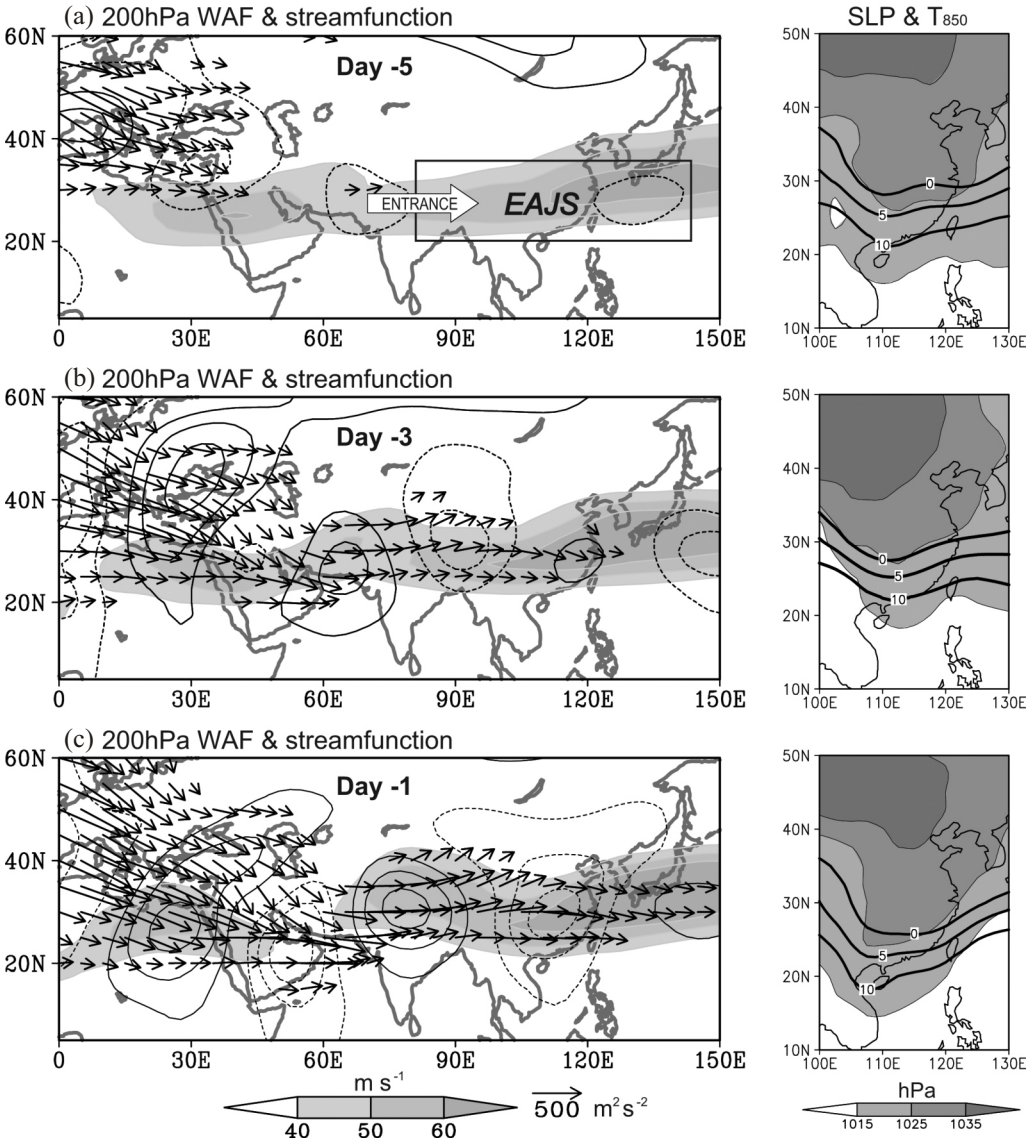

Fig. 5. Temporal evolution of 200-hPa wave activity flux and stream function anomaly (left panel), and 850-hPa temperature and surface pressure (right panel) at Day -5, -3, and -1 of cold surge case 1. The numbering of "Day" denotes the leading days relative to cold surge onset. Shading in the left and right panels represents the 200-hPa jet stream and surface pressure, respectively. The rectangular box in Fig. 5a indicates the EAJS and the entrance of EAJS is marked by the thick arrow.

over 20 - N. They are shown in the Hovmüller diagram of Fig. 6. It shows that the four major events of energy conversion occurred concurrently with the four cold surges after late December and the kinetic energy conversion, mainly contributed by the term $uv\ \bar{u}/\ y$, was positive over eastern China (100 - 120 E) during the four cold surge events. Although the relative contribution of the two energy conversion terms varied from case to case due to the variance of the subtropical jet, for example, the magnitude of the term $(v^2\ \ u^2)\ \bar{u}/\ x$ in case 4 was smaller than the other three cases, the disturbances in all four cases grew at the expanse of the kinetic energy of the mean flow, indicating the contribution of barotropic instability to cold surges.

It is also interesting to note that energy conversion peaks (~400 $m^2\ s^{-2}\ day^{-1}$ on average) near 110 E. This suggests that the disturbance can be significantly amplified near the entrance of EAJS, and it may explain why the magnitude of the upper northerly anomaly has a local maximum in southern China as shown in Figs. 2 and 3.

5. WAVEGUIDE EFFECT OF SUBTROPICAL JET STREAM

The results shown above suggest that the Rossby wave-like disturbances originating in the Mediterranean-Sahara help trigger the East Asia cold surges during the 2004/05

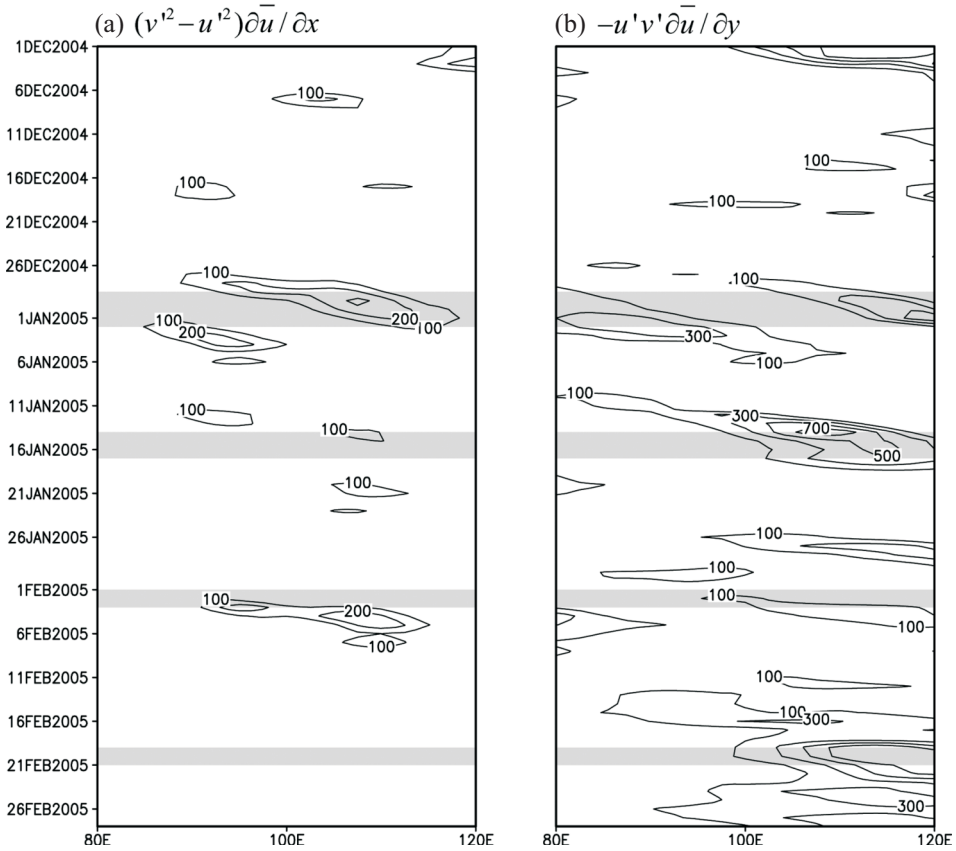

Fig. 6. Same as in Fig. 4, but for the barotropic kinetic energy conversion term, (a) $(v'^2 - u'^2)\,\partial\bar{u}/\partial x$, and (b) $-u'v'\,\partial\bar{u}/\partial y$. Only energy conversion larger than 100 $m^2\ s^{-2}\ day^{-1}$ is plotted. Contour interval is 100 and 200 $m^2\ s^{-2}\ day^{-1}$ for Figs. 6a and b respectively. Gray shading indicates the four cold surge events.

winter, and the EAJS is linked to the cold surges by acting as a waveguide and reinforcing the amplitude of the disturbances. This waveguide effect was simulated using the barotropic model described in section 2.

To show the waveguide effect of the basic flow on wave propagation, numerical experiments with the same forcing in three different basic flows, i.e., climz_exp, clim_exp, and surge_exp, were carried out. Note that December 2004 exhibited very different climatic characteristics from January - February 2005. Therefore, this study focuses on the latter period. The three basic flows are shown in Fig. 7 for comparison. It shows that the EAJS is significantly enhanced (zonal mean wind exceeds 55 m s^{-1}) in the surge_exp. The larger peak wind is accompanied by a larger meridional gradient, implying larger wind shear instability.

An examination of the upper-tropospheric divergence in January - February 2004/05 revealed a strong divergence anomaly over the Sahara (Fig. 8a); it was the strongest divergence anomaly in the Northern Hemisphere. Interestingly, the January - February meridional wind anomaly exhibits a clear wave-like pattern (Fig. 4) similar to the one shown in Fig. 5.

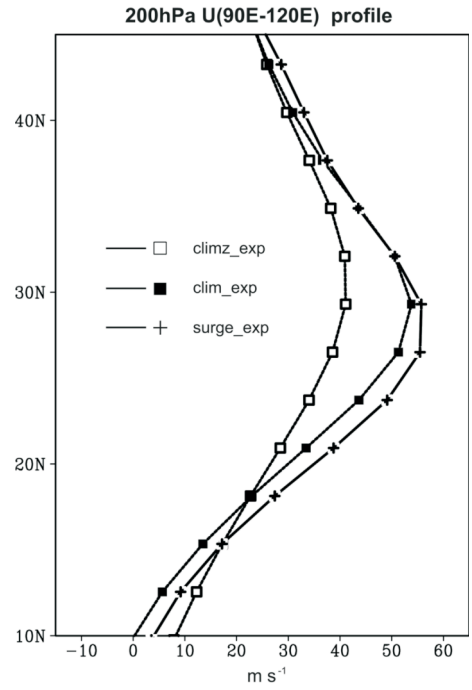

Fig. 7. Meridional profile of the 200-hPa zonal wind averaged over 90 - 120°E for the three basic flows: climatological zonal mean flow (climz_exp), climatological time mean flow (clim_exp), and mean flow in January - February 2005 (surge_exp).

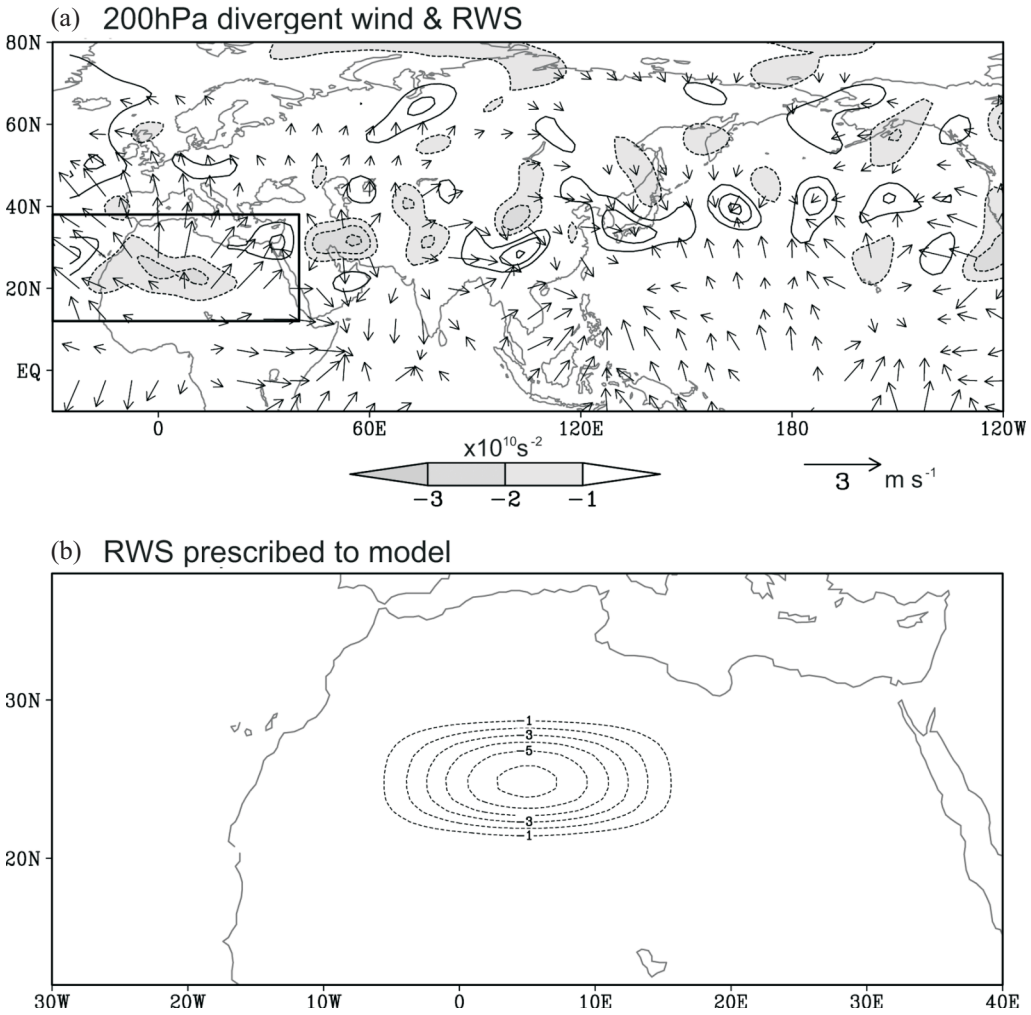

Fig. 8. (a) Distributions of the 200-hPa divergent wind anomaly and the RWS (shading) in January - February 2005; (b) An elliptical RWS prescribed in the barotropic model. The RWS shown has been multiplied by 10^{10}, and the contour interval is 1 s^{-2}. Rectangular box in (a) marks the domain shown in (b).

The RWS associated with the divergence over the Mediterranean-Sahara region was calculated (Fig. 8a) and a similar pattern was prescribed as forcing in the barotropic model (Fig. 8b). The steady responses of stream function to the prescribed RWS are shown in Figs. 9a - c. In the experiment of climatological zonal-mean flow, major disturbances forced near the Sahara propagate northeastward along a great-circle like path to Siberia and East Asia (Fig. 9a). Although disturbances also appear in the subtropical waveguide, their magnitude is very weak. In the climatological mean flow experiment (clim_exp), the northeastward propagation becomes much weaker, while the major disturbances propagate mostly eastward along the subtropical jet stream (Fig. 9b). Although the waveguide effect of the subtropical jet stream is much clearer in this experiment, the disturbance is still weak to the north of India, where the weak absolute vorticity gradient leads to energy leakage to the north. In the experiment of the January - February 2005 mean flow (surge_exp), there is almost no northeastward propagation (Fig. 9c). Almost all disturbances propagate eastward along the subtropical waveguide. Note the great similarity in the simulated wave-like pattern to the observed pattern shown in Fig. 5c. This contrast between surge_exp and clim_exp can be attributed to the westward extension of the EAJS during January - February 2005 to form a better defined waveguide. It is also interesting to note the enhancement of the anticyclonic circulation to the north of India, which results in a stronger northerly over eastern China. The distribution of barotropic kinetic energy conversion in the surge_exp experiment is similar to that observed (Fig. 10a). The local maximum of energy conversion located near 110°E reveals the amplification of disturbance in East Asia (Figs. 2, 3) by extracting kinetic energy from the basic flow, which is consistent with the Hovmüller diagrams of the observed barotropic kinetic energy conversion (Fig. 6).

6. CONCLUSION

This study explores the possible effect of upstream wave activity on East Asian cold surges that affected Taiwan in the 2004/2005 winter, and the waveguide effect of the subtropical jet stream. The major findings are:

a. Four cold surges in the 2004/2005 winter were preceded by upstream wave trains in the upper troposphere, which originated in the Mediterranean and Sahara and propagated eastward along the subtropical jet stream over

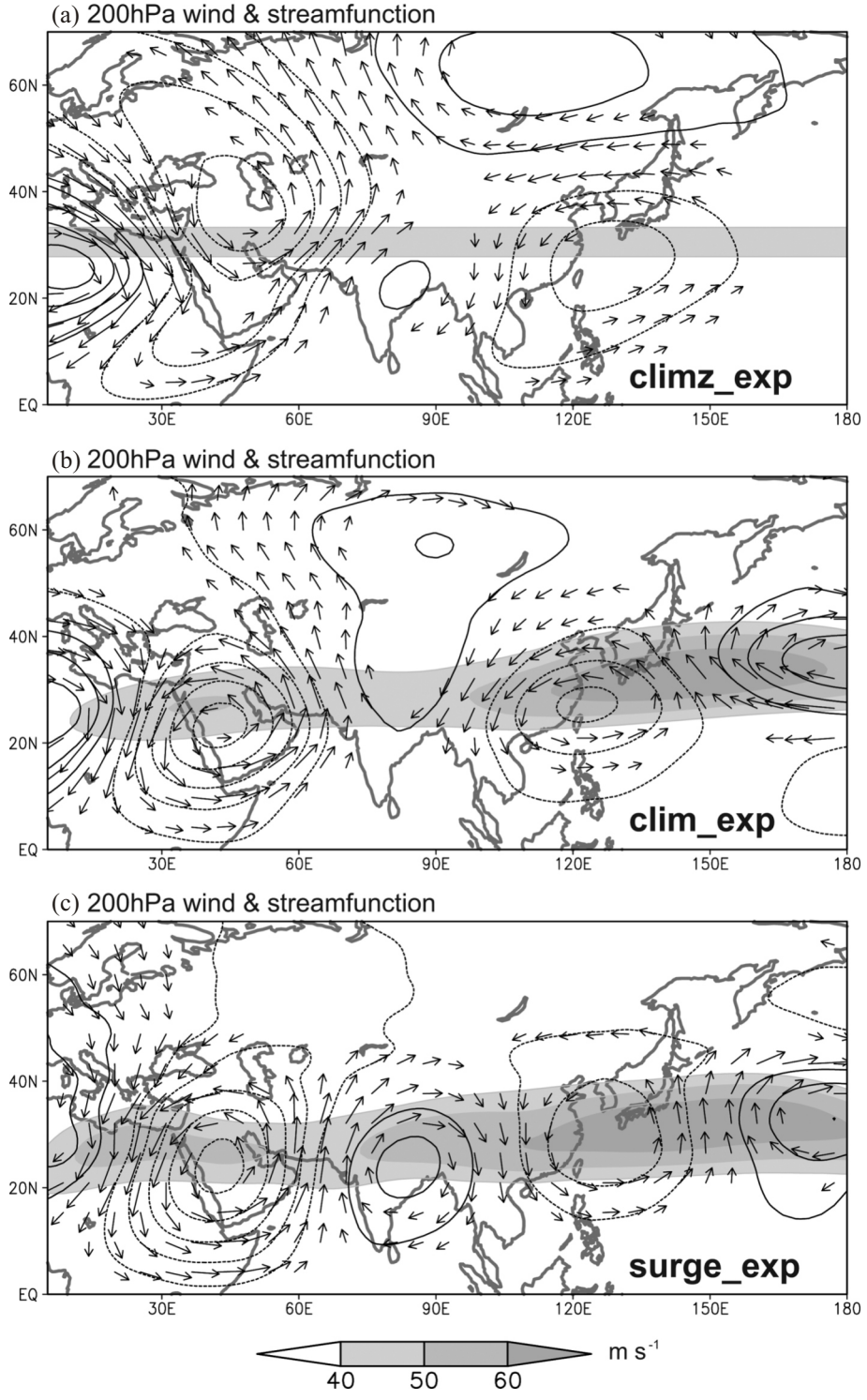

Fig. 9. Steady response (representing 200-hPa stream function anomaly) to the RWS as shown in Fig. 8b. (a) - (c) are simulated results of climz_exp, clim_exp, and surge_exp. Contour interval is 100 $m^2 s^{-1}$, and shading denotes 200-hPa zonal wind larger than 40 m s^{-1}.

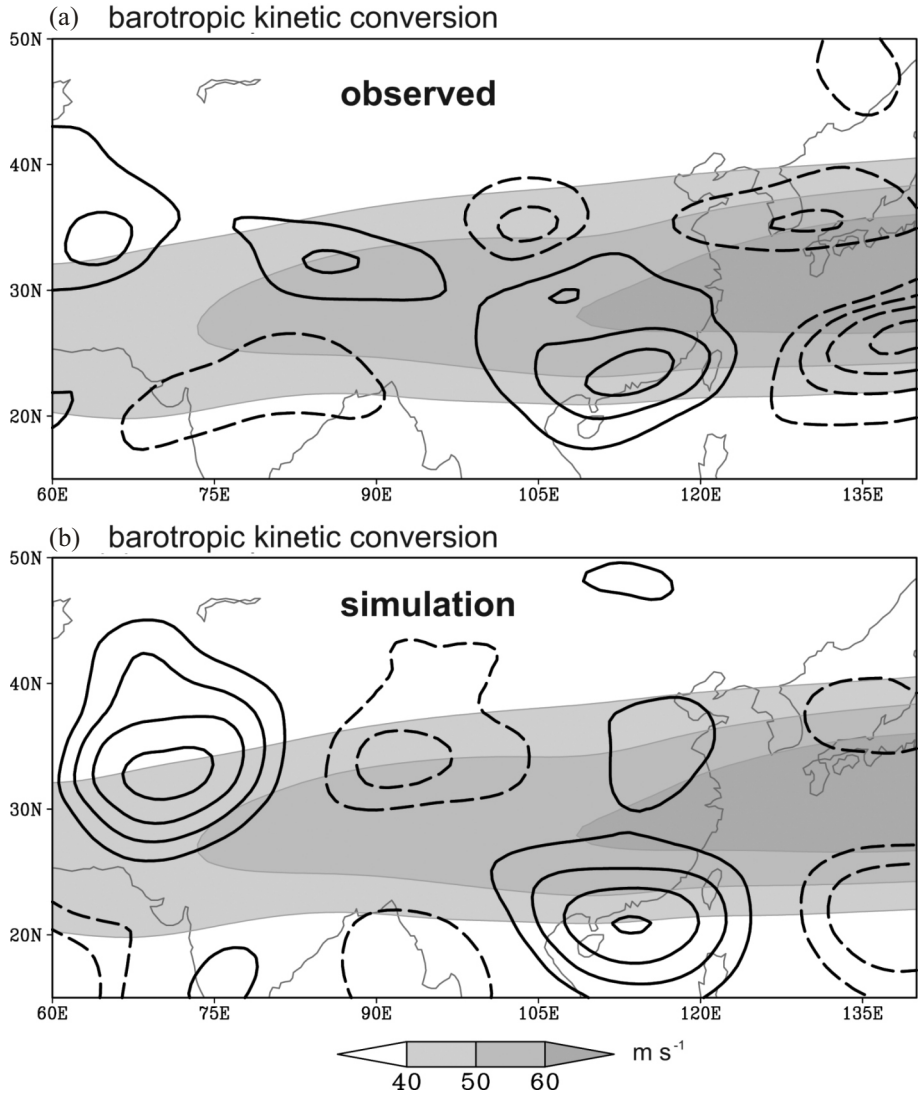

Fig. 10. (a) Observed and (b) simulated barotropic kinetic energy conversion. The shading indicates the 200-hPa zonal wind larger than 40 m s^{-1}. Contour interval is 100 and 10^{-8} m^2 s^{-2} day^{-1} for (a) and (b), respectively. Since the RWS is multiplied by 10^{-5}, the simulated number is much smaller than the observed.

the Eurasian continent. The northerly of the upper-level cyclonic anomaly in East Asia coupled with the low-level northerly upon the arrival of wave activity, followed by a quick southward penetration of cold air mass and surface anticyclone.

b. The results from the diagnosis and numerical experiments suggest that the anomalously active wave activity affecting the East Asian cold surges may be attributed to the anomalously enhanced jet stream over the Middle East and the anomalously westward extended EAJS. The configuration of these two subtropical jet streams established a strong waveguide through which the wave activity forced in the Mediterranean-Sahara region efficiently propagated to East Asia and resulted in more-than-average cold surge events in subtropical East Asia.

Watanabe (2004) pointed out that the Mediterranean-Sahara region is a key region for climatic fluctuation in the Atlantic, influencing the East Asian winter climate through the waveguide effect of the subtropical jet stream. This study demonstrates similar phenomenon on a synoptic time scale during a particular winter. Although it is not clear what factors lead to the anomalous subtropical jet stream in January - February 2005, the anomalously strong waveguide had apparently resulted in a shift of the preferred path for the Rossby wave energy dispersion that led to the anomalous behavior of the synoptic disturbances in East Asia during January - February 2005. How often and robust this mechanism affects cold surge activity in East Asia is an open question and is being investigated based on multi-year datasets.

Acknowledgements This study was supported by NSC

95-211-M133-001-AP4 and NSC-96-2745-M-002. The valuable suggestions of two reviewers are highly appreciated.

REFERENCES

Boyle, J. S. and T. J. Chen, 1987: Synoptic aspects of the winter time East Asian monsoon. In: Chang, C. P. and T. N. Krishnamurti (Eds.), Monsoon Meteorology, Oxford University Press, 125-160.

Chen, T. C., M. C. Yen, W. R. Huang, and W. A. Gallus, 2002: An East Asian cold surge: Case study. *Mon Wea. Rev.*, **130**, 2271-2290, doi: 10.1175/1520-0493(2002)130<2271:AEACSC>2.0.CO;2. [Link]

Compo, G. P., G. N. Kiladis, and P. J. Webster, 1999: The horizontal and vertical structure of east Asian winter monsoon pressure surges. *Quart. J. Roy. Meteor. Soc*., **125**, 29-54, doi: 10.1002/qj.49712555304. [Link]

Hoskins, B. J. and T. Ambrizzi, 1993: Rossby wave propagation on a realistic longitudinally varying flow. *J. Atmos. Sci*., **50**, 1661-1671 doi: 10.1175/1520-0469(1993)050<1661:RWPOAR> 2.0.CO;2. [Link]

Hsu, H. H., 1987: Propagation of low-level circulation features in the vicinity of mountain ranges. *Mon. Wea. Rev.*, **115**, 1864-1893, doi: 10.1175/1520-0493(1987)115<1864:POLLCF>2.0.CO;2. [Link]

Hsu, H. H., 1994: Relationship between tropical heating and global circulation: Interannual variability. *J. Geophys. Res*., **99**, 10473-10489, doi: 10.1029/94JD00247. [Link]

Hsu, H. H. and S. H. Lin, 1992: Global teleconnections in the 250mb streamfunction field during the Northern Hemisphere winter. *Mon. Wea. Rev.*, **120**, 1169-1190, doi: 10.1175/1520-0493(1992)120<1169:GTITMS>2.0.CO;2. [Link]

Joung, C. H. and M. H. Hitchman, 1982: On the role of successive downstream development in east Asian polar air outbreaks. *Mon. Wea. Rev.*, **110**, 1224-1237, doi: 10.1175/1520-0493(1982)110<1224:OTROSD>2.0.CO;2. [Link]

Kalnay, E., M. Kanamitsu, R. Kistler, W. Collins, D. Deaven, L. Gandin, M. Iredell, S. Saha, G. White, J. Woollen, Y. Zhu, M. Chelliah, W. Ebisuzaki, W. Higgins, J. Janowiak, K. C. Mo, C. Ropelewski, J. Wang, A. Leetmaa, R. Reynolds, R. Jenne, and D. Joseph, 1996: The NCEP/NCAR 40-year reanalysis project. *Bull. Amer. Meteor. Soc*., **77**, 437-471, doi: 10.1175/1520-0477(1996)077<0437:TNYRP>2.0.CO;2. [Link]

Lau, N. C. and K. M. Lau, 1984: The structure and energetics of midlatitude disturbances accompanying cold-air outbreaks over east Asia. *Mon. Wea. Rev.*, **112**, 1309-1327, doi: 10.1175/1520-0493(1984)112<1309:TSAEOM>2.0.CO;2. [Link]

Sardeshmukh, P. D. and B. J. Hoskins, 1988: The generation of global rotation flow by steady idealized tropical divergence. *J. Atmos. Sci*., **45**, 1228-1251, doi: 10.1175/1520-0469(1988)045<1228:TGOGRF>2.0.CO;2. [Link]

Simmons, A. J., J. M. Wallace, and G. W. Branstator, 1983: Barotropic wave propagation and instability, and atmospheric tele-connection patterns. *J. Atmos. Sci*., **40**, 1363-1392, doi: 10.1175/1520-0469(1983)040<1363:BWPAIA>2.0.CO;2. [Link]

Takaya, K. and H. Nakamura, 2001: A formulation of a phase-independent wave-activity flux for stationary and migratory quasigeostrophic eddies on a zonally varying basic flow. *J. Atmos. Sci*., **58**, 608-627, doi: 10.1175/1520-0469(2001)058<0608:AFOAPI>2.0.CO;2. [Link]

Watanabe, M., 2004: Asian jet waveguide and a downstream extension of the north Atlantic oscillation. *J. Climate*, **17**, 4674-4691, doi: 10.1175/JCLI-3228.1. [Link]

Wu, C. Y., H. H. Chia, and C. C. Hong, 2007: The long-term statistics of cold surge in Taiwan. Proceedings conference on Weather Analysis and Forecasting, May 15 ~ 17, 2007, Acer Aspire Park, Longtan , Taiyuan County, Taiwan.

Wu, M. C. and J. C. L. Chan, 1995: Surface features of winter monsoon surges over South China. *Mon. Wea. Rev.*, **123**, 662-680, doi: 10.1175/1520-0493(1995)123<0662:SFOWMS>2.0.CO;2. [Link]

Wu, M. C. and J. C. L. Chan, 1997: Upper-level features associated with winter monsoon surges over South China. *Mon. Wea. Rev.*, **125**, 317-340, doi: 10.1175/1520-0493(1997)125<0317:ULFAWW>2.0.CO;2. [Link]